Article

Solar UAVs—More Aerodynamic Efficiency or More Electrical Power?

Liviu Dinca, Jenica-Ileana Corcau * and **Daniel-Gabriel Voinea**

Department of Electrical, Energetic and Aerospace Engineering, Faculty of Electrical Engineering, University of Craiova, 200585 Craiova, Romania; ldinca@elth.ucv.ro (L.D.); voinea.daniel.s4a@student.ucv.ro (D.-G.V.)
***** Correspondence: jcorcau@elth.ucv.ro

Abstract: Solar UAVs (unmanned aerial vehicles) have experienced important development in recent years. The use of solar free energy is not neglected in the present energy crisis, with the intention to move toward green energies. However, an important problem arises concerning the limited amount of solar energy available on board UAVs. Until now, high-aerodynamic-efficiency configurations have been used. These configurations use high-aspect-ratio wings. However, high-aspect-ratio wings have some disadvantages regarding their excessive elasticity and weak bending resistance in the housing section. Additionally, the aircraft maneuverability is reduced. In this work, a study is proposed on a solar UAV configuration that sacrifices high aerodynamic efficiency for a higher surface area available for solar cells. In this manner, the amount of energy available on board the UAV is increased, and the UAV structure becomes more rigid and robust. The presented UAV fits better with more complex evolutions, is more maneuverable and the wingspan is much reduced. This UAV is more compact, can maneuver better in the take-off and landing phases, and the necessary storage space is considerably reduced. This paper highlights the performances that can be achieved using this kind of UAV and explores whether these performances are enough for some applications. Using an on-board energy balance, the possible performances of this new configuration is studied. As this is a preliminary study, the precision level is not very high, but it offers an image concerning the possibilities of this new configuration.

Keywords: UAV; aerodynamic efficiency; electrical power

1. Introduction

It is well known at present that society needs to move away from fossils fuel energy toward green energies. One of these energies is solar energy, and its implementation in aviation is an interesting research topic currently. However, there are some problems concerning solar energy in UAVs. The greatest problem is the very limited amount of energy possible to be obtained on a UAV using solar cells. It is well known the maximum solar radiation on the ground is around 1000 W/m^2, and it increases by several percent at higher altitudes. The energetic efficiency of the best performing solar cells is around 25–30%, and this is obtained using silicon mono-crystalline solar cells. Optimistically speaking, the amount of energy possible to be obtained is around 250–300 W/m^2. A light airplane such as a Cessna 172 has a 16.17 m^2 wing surface and 134 kW engine power. Taking into account the previous data and supposing that the entire wing is covered with solar cells, it is possible to obtain a maximum of 4.84 kW of electrical power. With 25% supplementary energy using fuselage- and empennage-mounted solar cells, this comes to 6.06 kW in total. This represents only 4.5% of a Cessna 172's engine power. Additionally, this power can be obtained only at maximum solar radiation. Solar radiation changes significantly throughout the day, from dark in the night to the maximum at noon. In conclusion, it can be said that the solar energy available is not enough for commercial applications in aviation.

Special applications such as experimental UAVs for surveillance and even pseudo-satellites have been studied. UAVs and even manned aircraft (with one person) with propulsion based only on solar power have been built. All of these applications have the overall configuration in common. They follow a maximum aerodynamic efficiency and, by consequence, high-aspect-ratio wings. Many studies have been performed in this direction [1–8]. Experimental studies have been performed on these configurations [9] and numerical multi-physics simulations [10]. The experience of a flight around the world on a solar aircraft was described in [11]. As was expected, based on the aerodynamic principles, all of these studies led to a high-aspect-ratio wing of the aircraft. This configuration ensures maximum aerodynamic efficiency. This type of UAV includes Atlantik Solar, developed at the University of Zurich (Figure 1a [1]); Sky Solar, smaller and also developed at the University of Zurich (Figure 1b [2]); and the Sun project, developed at the University of Hong Kong (Figure 1c [3]). These are relatively small UAVs with wingspans between 2 and 6 m. A stratospheric airship with electric motors fed from solar cells was proposed in [4] (Figure 1d). However, large-scale projects were also developed in this period, including pseudo-satellites such as Zephir from Airbus (Figure 1e) [10] and ELHASPA from DLR (Figure 1f) [10]. These projects are aircraft with wingspans of tens of meters. Despite their large wingspan, their payload is small. For example, the Zephir 8 project weighs 60 kg, has a 25 m wingspan and a 5 kg payload.

(**a**)

(**b**)

(**c**)

(**d**)

(**e**)

(**f**)

Figure 1. *Cont.*

(**g**)

(**h**)
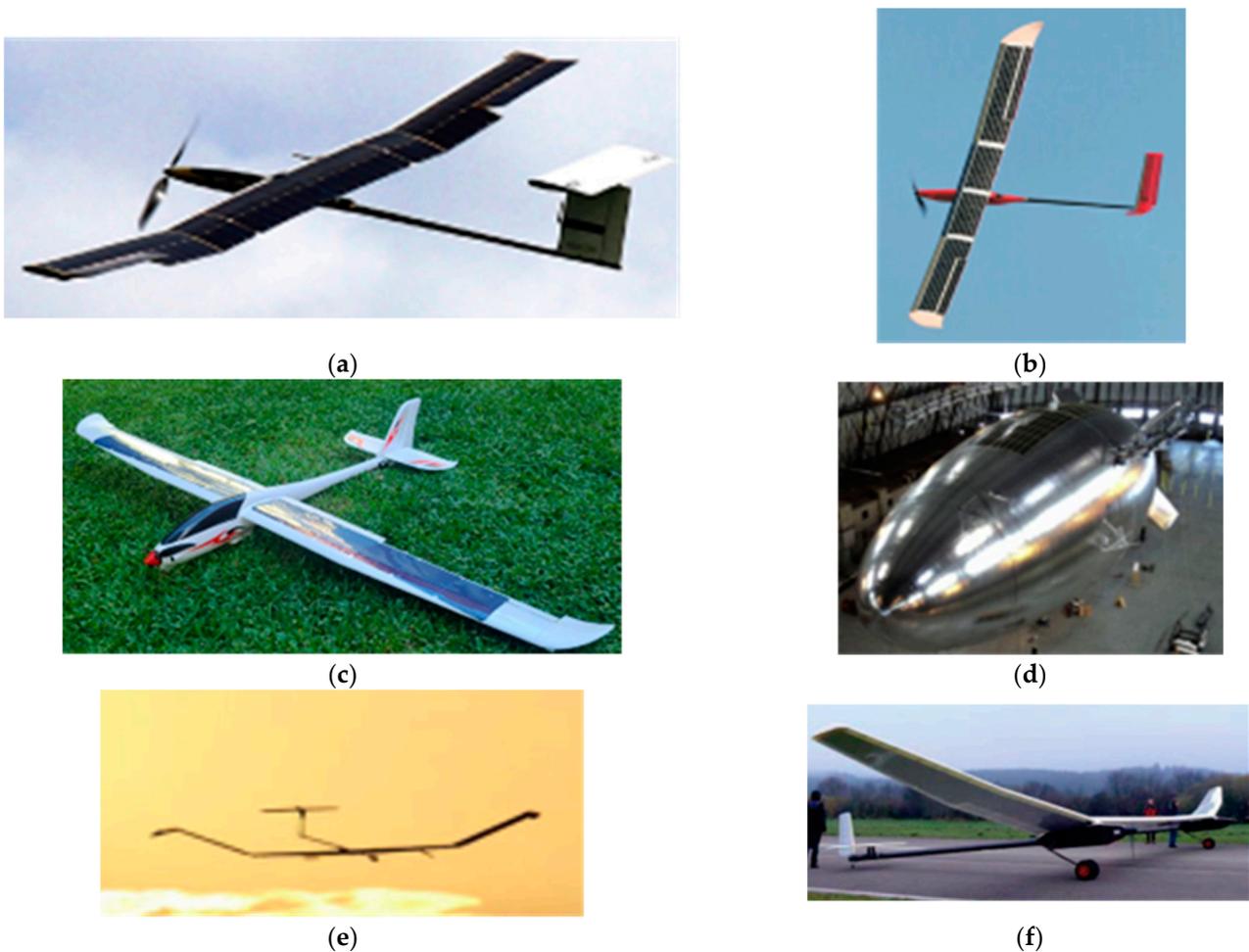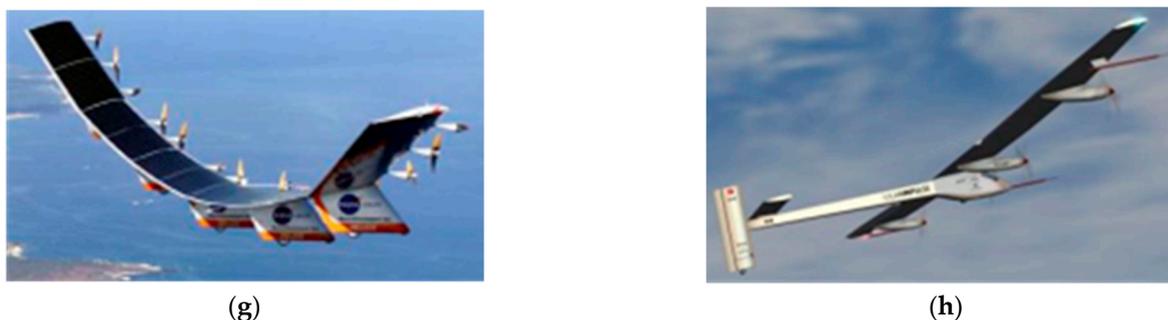
Figure 1. Different solar UAVs and aircraft. (**a**) Atlantik Solar from Zurich University; (**b**) Sky Solar from Zurich University; (**c**) Sun project from Hong Kong University; (**d**) Stratospheric airship, solar powered; (**e**) Zephir project from Airbus; (**f**) ELHASPA project from DLR; (**g**) Helios project from NASA; (**h**) Solar Impulse project.

Large aircraft with wingspans of tens of meters also include Helios (Figure 1g [2]) and Solar Impulse (Figure 1h [2]). The Helios project has a 75 m wingspan and weighs 726 kg. The project Solar Impulse has a 72 m wingspan, weighs 2.3 tons and carries a one man crew. All of these UAVs and aircraft were designed for research purposes and to beat the altitude or flight time records of their time. Flight time grew from a few hours to a few days of continuous flight. Future research will build pseudo-satellites with five-year flight time.

The defining characteristic of these aircraft is their large wingspan, low weight and high-elasticity structure. The huge deformation of the Helios aircraft can be observed in Figure 1g. These high stresses led to the in-flight disintegration of the aircraft in 2003.

In order to reach a very low weight for these aircraft, modern composite materials based on carbon fiber and Kevlar are used. Their high resistance capabilities with respect to classical aviation alloys are exploited to the maximum. Trying to reduce the structure weight as much as possible can lead to an exaggerated elasticity. The aircraft integrity is therefore in danger in some closed evolutions. Only the Solar Impulse project has higher rigidity. It was designed to fly around the world with a man on board, and so special attention was paid to its flight safety. Its structure weighs 2.3 tons with a 72 m wingspan, 3 times heavier than Helios with a 75 m wingspan.

These configurations have some important disadvantages in addition to the structural strength being reduced to minimum and the exaggerated elasticity. Atmospheric currents significantly influence an aircraft's flight, causing reduced maneuverability. This is the price paid by designs aimed at breaking world records.

Studies concerning solar aircraft are presented in [12,13].

The experience gained in these projects led to the conclusion that flight using only solar energy is very difficult to realize. Gradually, these studies moved toward hybrid propulsion based especially on batteries and solar cells or batteries, solar cells and fuel cells. In this case, it is useful to have very good power management between the power sources on board. This kind of study can be found in [14–16]. In addition to studying power management systems, [17] studied the solar cell matrix for UAVs through numerical simulations. An optimization of electric motors used for UAVs is descried in [18]. Authors will continue to seek superior-performance electrical motors to be used on UAVs.

In addition to [4], there are other studies proposing airships with electrical motors driven by solar energy (see [19]).

Better energy management on board can be sustained by aircraft trajectory optimization. Important studies appeared in this field—see [20,21]. Experimental studies on UAVs are presented in [22].

An interesting review concerning many aspects linked to the UAV domain can be found in [23]. This review discussed the possibility of using different UAV configurations, their performance, communication possibilities, battery recharge systems, security issues and so on.

Based on these results, the studies concerning solar aircraft are very advanced, and more and more new developments continue to appear. Researchers are gradually discarding studies concerning the design of aircraft for breaking world records using solar energy. Attention is focusing more and more on hybrid propulsion systems to save as much energy as possible using solar cells alongside other energy sources. It seems that this is the most realistic direction for using solar energy in aviation. Optimizations of different aspects of solar aircraft or hybrid-propulsion aircraft are the object of the most recent studies in this field.

In the following, a new configuration of solar airplane is proposed. Then, the horizontal flight and climb performance are studied using the available and necessary power method. Additionally, a configuration for the electrical on-board system is defined and an estimation of its function is provided using MATLAB/Simulink simulation. In this work, the performance obtained with the new configuration is compared with the performance of a solar airplane with a high-aspect-ratio wing.

2. A New Configuration of a Solar Cell UAV

All the studies mentioned in the previous section were oriented toward designing solar UAVs with the maximum aerodynamic efficiency, neglecting structural robustness and maneuverability. In this way, solar aircraft with a high wingspan and very low payload were designed. Solar Impulse has a 72 m wingspan and can carry one single person; meanwhile, a Boeing 747 has a 70 m wingspan and carry over 350 persons.

This work proposes a solution to decrease the dimensions (namely the wingspan) of solar UAVs. It is not suggested that this configuration will reach the performance of UAVs presented in the introduction, but the capabilities offered by this configuration are explored.

This study started from the configuration of the *Creative Aircraft* UAV. This aircraft was built at the University of Craiova. Its configuration is presented in Figure 2. In the following, this configuration is referred to as the glider configuration. This glider is a UAV with a 3 m wingspan, a 1.2 m length, a 0.26 m housing chord, a 2.2 kg mass and 40 solar cells on board on the upper face of the wing. This represents the maximum possible number of solar cells for this configuration. The wing airfoil is FX 63-120 and the horizontal empennage airfoil is NACA 0008.
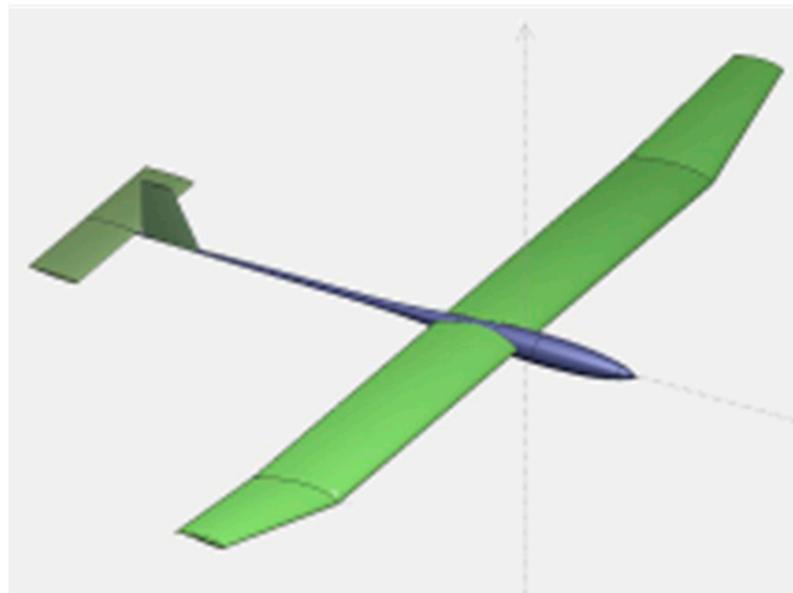
Figure 2. *Creative Aircraft* configuration (glider configuration).

The authors sought to obtain an UAV with the same wingspan as this glider configuration, but also to increase the solar energy produced by the solar cells as much as

possible. This meant increasing the upper flat surface of the UAV. The wing chord and the empennage chord were increased and a configuration of a lifting fuselage with a flat upper surface was adopted. A first sketch of the top view is shown in Figure 3 [24]. The authors succeeded in placing 136 solar cells on the UAV, nearly 4 times more than on the glider configuration. The available energy will increase proportional to the number of solar cells. The authors refer to this configuration as the *Newsolar* configuration.
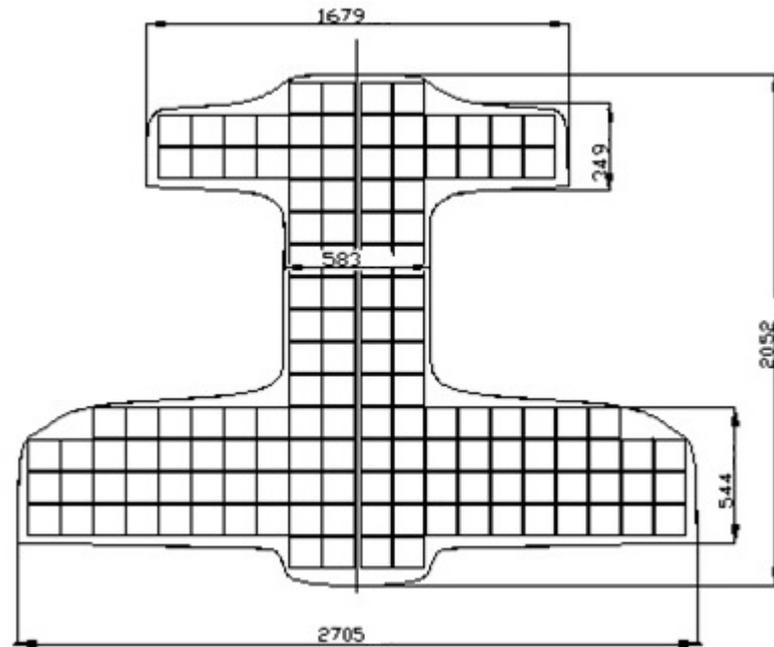
Figure 3. Solar cells disposition on the upper surface of *Newsolar*.

In order to improve the global lift of the UAV, a lifting fuselage configuration was adopted, with a "T" section, as shown in Figure 4.
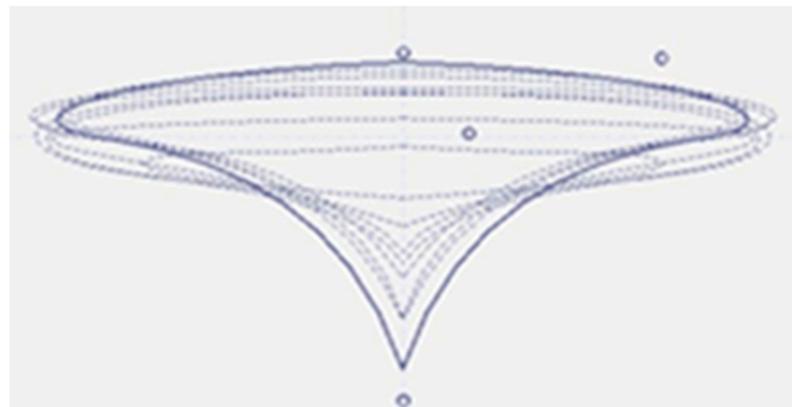
Figure 4. Fuselage section of the *Newsolar*.

The authors adopted a canard configuration. It is well known that this configuration offers better aerodynamic qualities than a classical empennage. In a canard configuration, both the wing and horizontal empennage have positive lift. The UAV's global lift is the sum of the wing lift, horizontal empennage lift and fuselage lift in this case. In the classical configuration, the horizontal empennage has usually a negative lift. The global lift of the UAV is the difference between the wing lift and the horizontal empennage lift. This is the reason why the configurations in Figure 1 have a very small horizontal empennage with

respect to the wing, placed at a great distance from the wing. The horizontal empennage provides a small amount of negative lift and decrease the global lift very slightly with respect to the wing lift. The great distance of the horizontal empennage from the center of gravity produces enough of a pitch moment for the aircraft to achieve longitudinal equilibrium.

All of these considerations led to the configuration modelled in XFLR 5 and presented in Figure 5. Some solutions were used in this configuration (as presented above) to improve the global lift of the UAV. The wing aspect ratio, however, remains small (around 5), unlike the configurations above 20 for the aircraft in Figure 1. It is not suggested that adopting these solutions will compensate for the losses in aerodynamic efficiency, but the purpose is to improve the performance as much as possible.
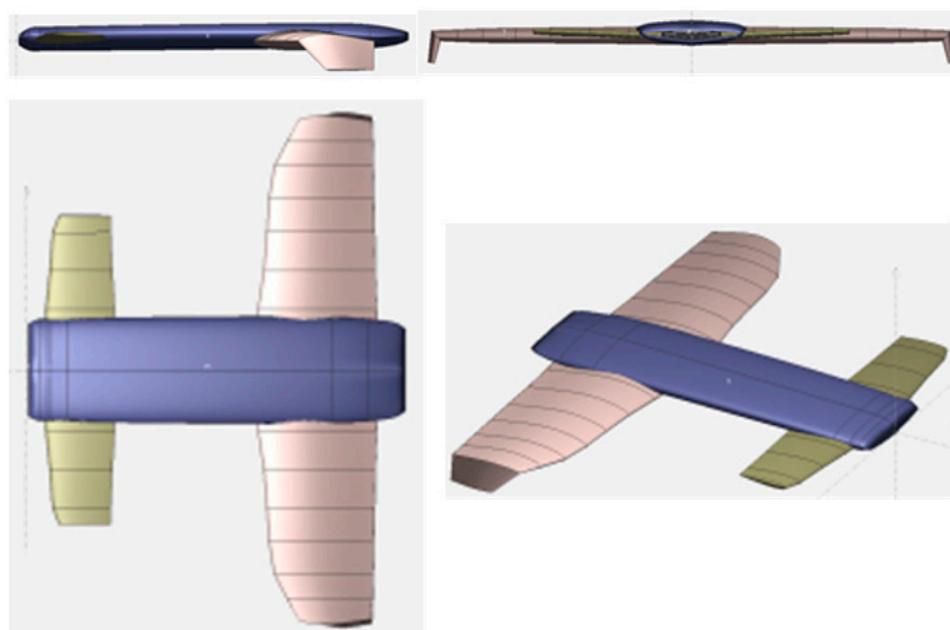
Figure 5. Configuration of *Newsolar*.

In order to avoid shading the upper surface solar cells, vertical empennages are removed from the wing tip and oriented downward instead. This represents a vulnerability of the aircraft in the take-off and landing phases. It thus requires higher landing gear (not presented in Figure 5), but the fuselage configuration also requires a higher landing gear, so this inconvenience is accepted.

The airfoil is NACA 64-215 both for the wing and horizontal empennage. The geometrical data for *Newsolar* are in Table 1.

Table 1. Geometrical data for *Newsolar*.

	Wing	**Horizontal Empennage**
Span (m)	2.71	1.68
Surface (m^2)	1.62	0.6
Mean aerodynamic chord	0.587	0.36
Aspect ratio	5.9	4.68

Using XFLR 5, the aerodynamic qualities for the both configurations are estimated—glider and *Newsolar*. These are presented in Figure 6.
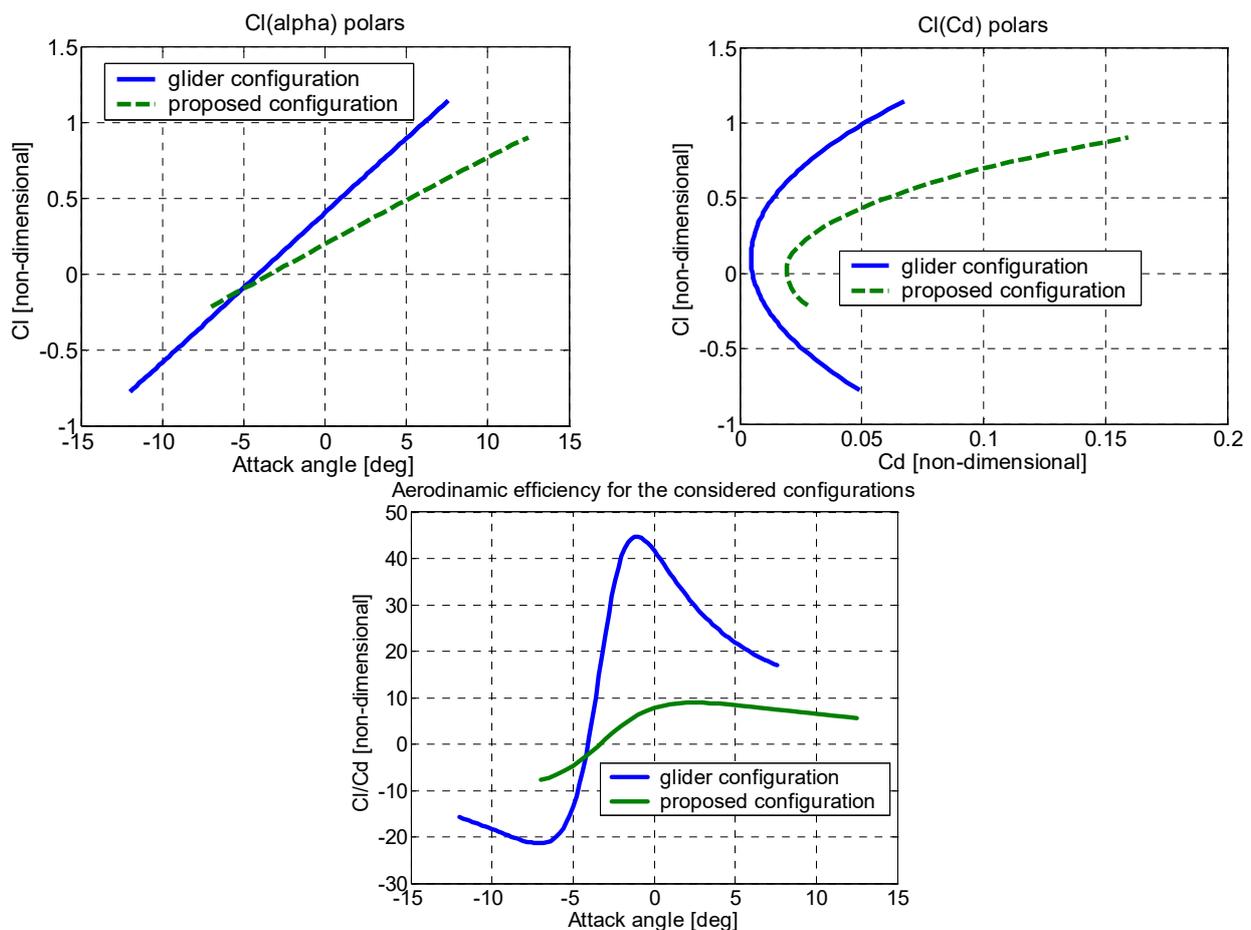
Figure 6. Aerodynamic polars for glider and *Newsolar* configurations.

It can be observed that *Newsolar* presents a lower lift and a higher drag. This means that it obviously has less aerodynamic efficiency. The authors therefore seek to establish the effect of this lower aerodynamic efficiency, taking into account the fact that *Newsolar* has a bigger surface are and four times more electrical energy.

An estimation of *Newsolar's* mass was provided in [24]: "we supposed the skin, for wing, horizontal empennage and fuselage consists in two layers of carbon fiber fabric with 80 g/m² density. Total surface of top projection is around 3.84 m². Supposing doubled this surface results 7.68 m² carbon fiber covered surface. Taking into account there are two layers results 1.228 kg carbon fiber. It was considered 1:1 ratio carbon fiber/epoxydic resin. Total 2.457 kg outer structure mass. Supplementary, it was considered a reinforcement internal structure, consisting of spars and ribs, with 700 g mass. Other elements: main gear legs 2 × 300 g, nose leg 150 g, battery 400 g, solar cells 884 g, electric motors 2 × 150 g, receiver, servos and other components 250 g. Entire total 5.741 g. It seems a realistic estimation taking into account the aircraft dimensions. It was supposed only 400 g battery because it is used mainly on take off and in closed man oeuvres in the rest of the time the aircraft is driven by solar energy."

For solar cells, the same solar cells were used as for *Creative Aircraft* (Maxeon C60) solar cells with 3.42 W output power and 22.5 efficiency, one of the highest atpresent. The mass of one solar cell was 6.5 g. The solar cell dimensions were 125 × 125 mm. The total output power for the 136 solar cells was465 W. For *Creative aircraft*, 40 solar cells offer only 136 W of output power. The solar cells Maxeon C60 are mono-crystalline silicon solar cells and have the advantage of being flexible. Even when small cracks appear in the bending process, the solar cell remains functional until it is completely cracked.

3. Performances Comparative Estimation

In order to obtain a more conclusive comparison between the possible configurations, *Creative Aircraft* was scaled up two times, so that it could receive 136 solar cells on the upper surface of the wing. This meant a 4-fold surface increase and the wingspan increased 2-fold. This configuration will be referred to in the following as the scaled glider configuration, and it has a 6 m wingspan. It is supposed that the aircraft's mass increases proportionally with the aircraft's surface area. So, from the 2.2 kg glider mass, it reached an 8.8 kg glider mass and 465 W of electrical power on board. The aerodynamic polars were considered the same as the *Creative Aircraft* polars, presented in Figure 6. Aerodynamic polars are modified with respect to the Reynolds number, but in this case we can neglect this variation.

In conclusion, we compare three configurations: glider, *Newsolar* and scaled glider. Their characteristics are presented in Table 2.

Table 2. Constructive data for the compared configurations.

	Glider	Newsolar	Scaled Glider
Span (m)	3	2.7	6
Wing surface (m^2)	0.725	1.7	2.9
Number of solar cells	40	136	136
Solar cells output power (W)	136	465	465
On-board equipment's consumed energy (W)	15	50	50
Power consumed for propulsion (W)	76	275	275
Propulsion power in cruise mode (W)	54	192	192
Loading batteries electrical power (W)	45	90	90
Electric motor maximum power (W)	350	700	700
Maximum propulsion power (W)	233	465	465
Aircraft mass (kg)	2.2	5.74	8.8
Payload mass (kg)	0.766	2	2
Total mass (kg)	2.966	7.74	10.8

The payload was considered to be 2 kg for *Newsolar* and for the scaled glider. For the glider configuration, it was considered to be the same percentage of aircraft mass as *Newsolar* that means around 35% of aircraft mass.

Regarding the power distribution, around 11% of energy from the solar cells was consumed by the on-board equipment in the glider configuration. For *Newsolar*, this was around 21%. From the remaining power, in a cruising regime, some of the power is used for battery loading and some is used for propulsion. However, the propulsion power is not the same as the electrical power of the electric motor. The electric motor has around 95% efficiency and the propeller has around 70% efficiency. It the propeller efficiency is considered constant, even when it is modified with respect to the flight regime.

The electric motor is fed at its maximum power using energy from the solar cells and batteries simultaneously. In this case, it is important that the electrical motor operates at maximum power. The glider configuration has one motor with a maximum power of 350 W. The other two configurations have two motors of the same type, so the electric motors' maximum power is 700 W. Considering electric motor efficiency and propeller efficiency, this provides 233 W propulsion power for the glider configuration and 465 W for the other two configurations.

3.1. Horizontal Flight Performances

Using the available and necessary power method, we calculated the performance of the three configurations.

The necessary power for a horizontal flight is

$$P_{nec} = \frac{\rho V^3}{2} S C_d,$$ (1)

the flight speed for a lift coefficient is

$$V = \sqrt{\frac{2mg}{\rho S C_l}}$$ (2)

and thus the necessary power for a horizontal flight is

$$P_{nec} = \sqrt{\frac{2}{\rho S}} (mg)^{3/2} \frac{C_d}{C_l^{3/2}}$$ (3)

For the glider configuration, the results obtained for the necessary power and available power are presented in Figure 7a, those for *Newsolar* are depicted in Figure 7b and those for the scaled glider are presented in Figure 7c. The necessary power for both an empty and loaded UAV is considered. At a low flight speed, a slight difference appears between the two situations, but for higher flight speeds, this difference vanishes. This difference is considerably higher for *Newsolar* due to its lower aerodynamic efficiency.
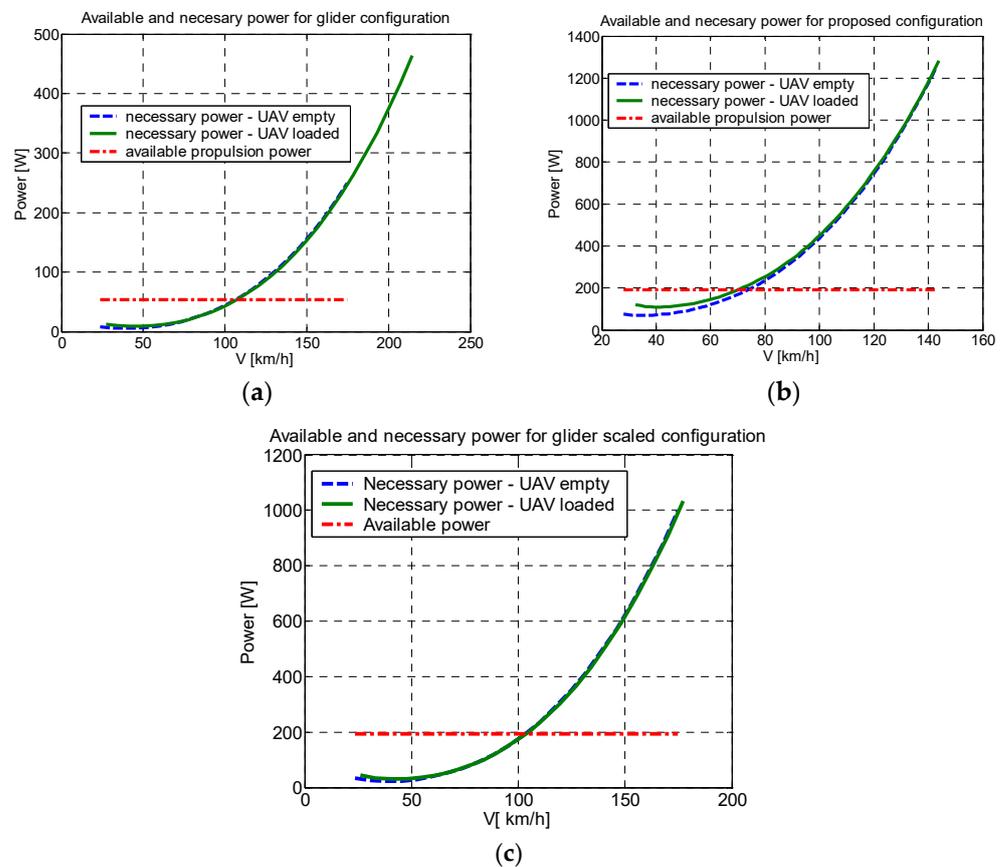
Figure 7. Available and necessary power for horizontal flight: (**a**) glider configuration; (**b**) *Newsolar* configuration; (**c**) scaled glider configuration.

In Table 3 it is observed for the scaled glider that the horizontal flight performance changes slightly with respect to the performance of the glider configuration. A greater difference appears in the maximum speed with the maximum electrical motor power. As is expected, the horizontal flight performance decreases for *Newsolar*. The maximum horizontal flight speed decreases, but it remains at an acceptable value. The minimum flight speed increases, but not by very much. Taking into account the advantages in structural rigidity and maneuverability, it can be said that this configuration is interesting for some applications.

Table 3. Minimum and maximum flight speeds.

	Glider	Newsolar	Scaled Glider
Minimum speed (km/h)	28	32	26
Maximum speed only solar cells (km/h)	107	74	116
Maximum speed at maximum electrical motors power (km/h)	170	102	135

Here, we highlight that the maximum speed for the glider configuration and for the scaled glider configuration is obtained from a power balance. In fact, these configurations have very elastic structures and it is possible that their maximum speeds will be limited to lower values due to aero-elastic considerations.

All of these studies apply to 0 m altitude in standard atmosphere.

3.2. Climbing Performances

The necessary power in a climbing flight is

$$P_{nec\gamma} = \frac{\rho V^3}{2} S C_d + mgV \sin\gamma \tag{4}$$

In this situation, the flight speed on a climb slope γ is

$$V = \sqrt{\frac{2mg\cos\gamma}{\rho S C_l}} \tag{5}$$

Because the climb slope is small for these aircraft, it can be approximated as $\cos\gamma = 1$, so the flight speed on the climb slope γ can be approximated with Equation (2). The necessary power for the climb on slope γ becomes

$$P_{nec} = \sqrt{\frac{2}{\rho S}}(mg)^{3/2}\frac{C_d}{C_l^{3/2}} + mg\sin\gamma\sqrt{\frac{2mg}{\rho S C_l}} = mg\sqrt{\frac{2mg}{\rho S}}\left(\frac{C_d}{C_l^{3/2}} + \frac{\sin\gamma}{\sqrt{C_l}}\right) \tag{6}$$

Using the same necessary and available power method, we obtained the results presented in Figure 8. The graphs in Figure 8 were considered for climb slopes between 0 and 30 degrees with 2-degree steps. Aircraft masses were considered only for the loaded situation. Based on the results in Figure 8, we obtained the climb characteristics presented in Figure 9. The graphs in Figures 8 and 9 apply to for climbing at the maximum electrical motor power. Considering climbing with the power offered by solar cells in the same conditions as horizontal flight, we obtained the results presented in Figures 10 and 11, respectively. The slopes and loads of the aircraft were the same as in Figures 8 and 9.

From the presented graphs, the maximum climbing speed at 0 m altitude is presented in Table 4.

Table 4. Maximum climbing speeds.

	Glider	Newsolar	Scaled Glider
Maximum climbing speed only with solar cells (m/s)	1.5	1	1.5
Maximum climbing speed with maximum electrical motor power (m/s)	7.5	4.5	4
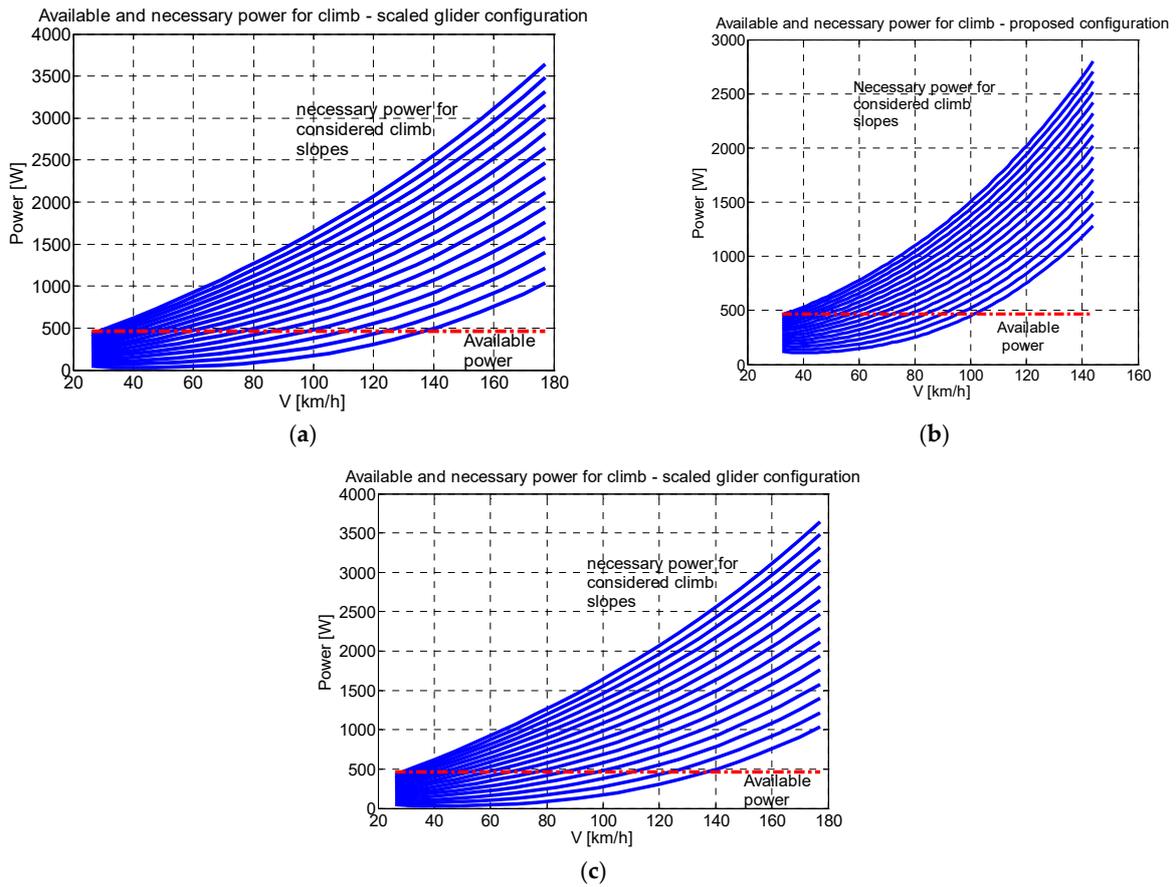
Figure 8. Necessary and available power for climbing at maximum electrical motor power: (**a**) glider configuration; (**b**) *Newsolar* configuration; (**c**) scaled glider configuration.

Figure 9. *Cont.*

(c)
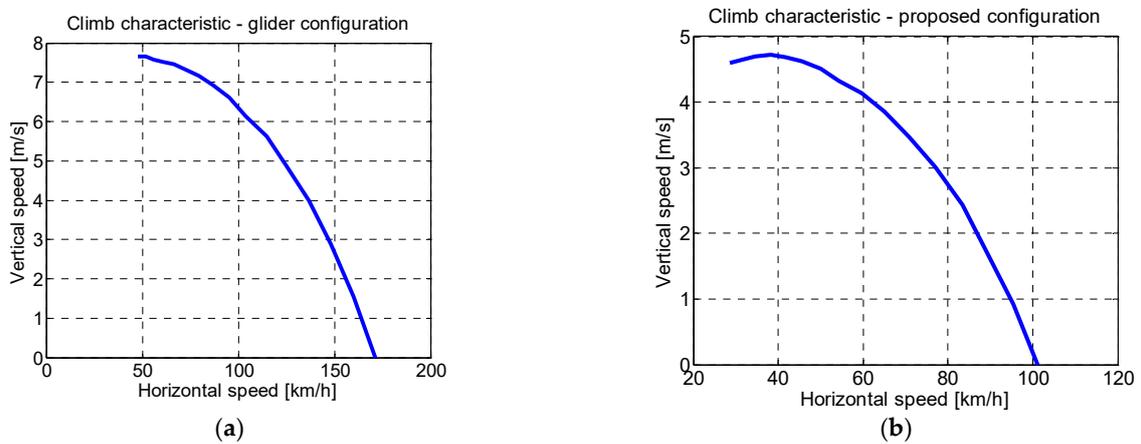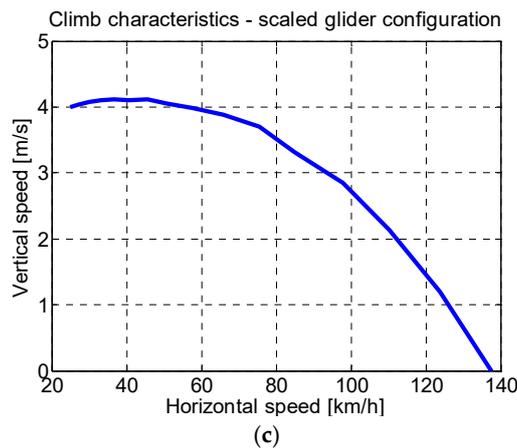
Figure 9. Climbing characteristics at maximum electrical motor power: (**a**) glider configuration; (**b**) *Newsolar* configuration; (**c**) scaled glider configuration.

(a)

(b)

(c)
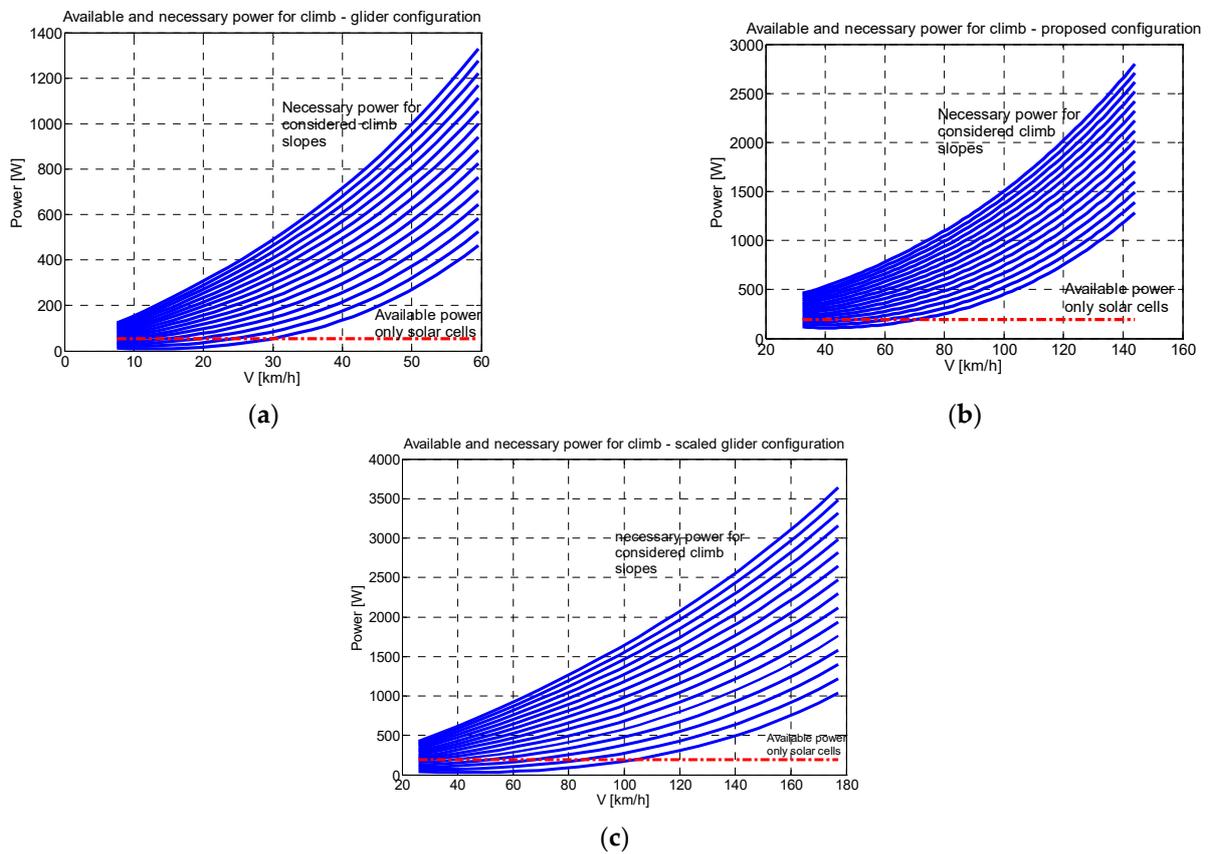
Figure 10. Necessary and available power for climbing using only solar cells: (**a**) glider configuration; (**b**) *Newsolar* configuration; (**c**) scaled glider.

In Table 4, an interesting fact can be noted. By scaling the glider configuration in order to obtain the same electrical power from solar cells, the climbing characteristics decay considerably. The maximum climbing speeds are almost equal to those for *Newsolar*. From this point of view, *Newsolar* is better. It is more convenient to build a smaller aircraft that is more compact, lighter and has the same payload.
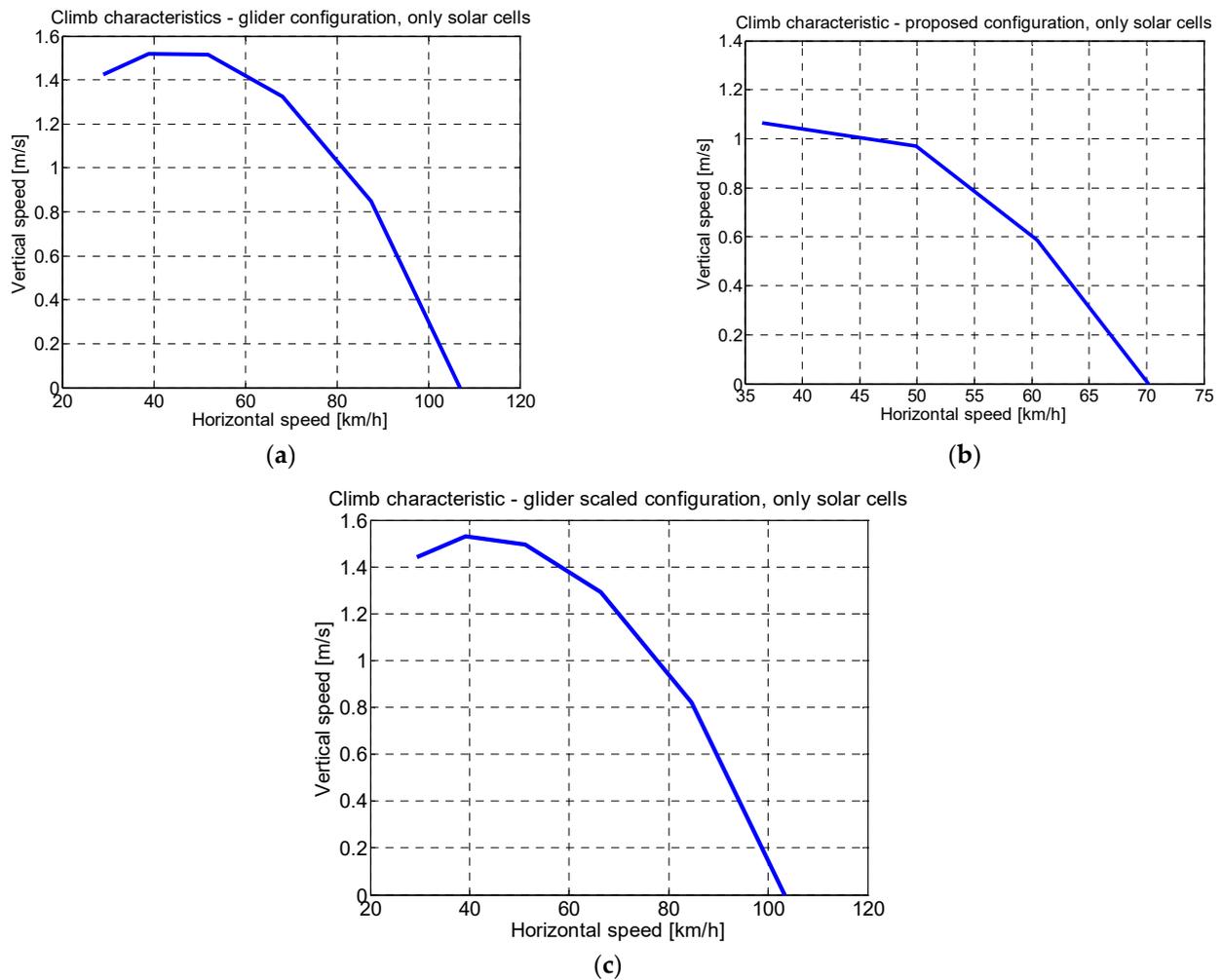
Figure 11. Climbing characteristics using only solar cells: (**a**) glider configuration; (**b**) *Newsolar* configuration; (**c**) scaled glider configuration.

3.3. Gliding Characteristics

Concerning the gliding characteristics, the relation is

$$tg\gamma_{\min} = arctg\left(\frac{1}{(C_l/C_d)_{\max}}\right) \tag{7}$$

Using the data in Figure 1c, the minimum gliding slopes are presented in Table 5.

Table 5. Minimum gliding slopes.

	Glider	**Newsolar**	**Scaled Glider**
$(C_l/C_d)_{\max}$	45	9	45
$\gamma_{\min}[^o]$	1.3	6.4	1.3

The glider configuration has an obviously better gliding performancs. *Newsolar*, in the absence of propulsion power, has a large descending slope, but this can be accepted if the idea is to obtain a more compact and maneuverable aircraft.

4. Electrical Systems Configuration

As was mentioned before, the on-board electrical systems for this kind of UAV with solar cells are, in fact, hybrid. They usually have as their electrical power sources either solar cells and batteries or solar cells, batteries and fuel cells [14–16]. For the aerodynamic configurations considered previously, a hybrid system with solar cells and a battery is chosen. The battery sustains the electrical system in take-off and climbing. After that, in cruise mode, the batteries are charged using some of the energy from the solar cells. The ensemble configuration of the on-board electrical system is the same for all of the studied configurations, but the components' parameters are different. This configuration modelled in Simulink is presented in Figure 12.
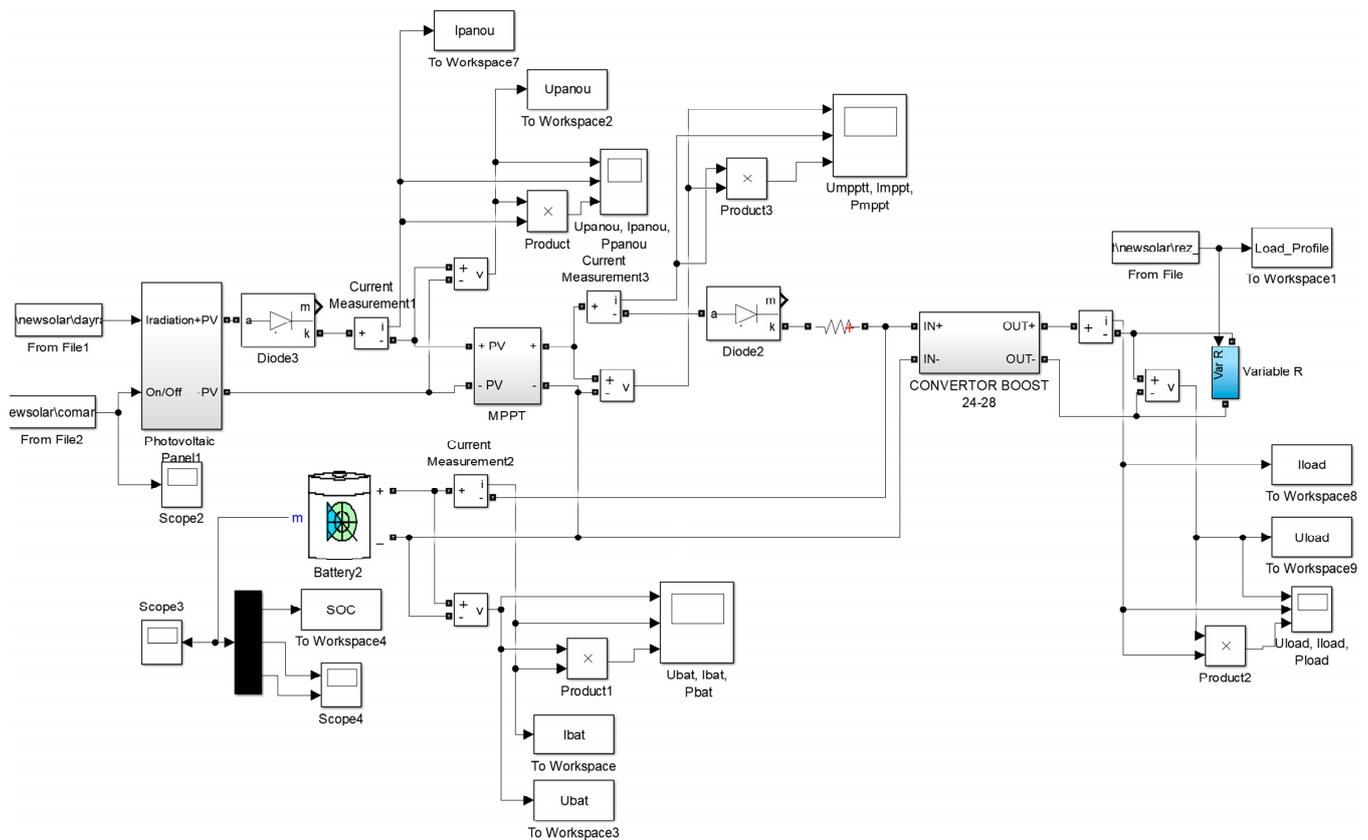
Figure 12. Hybrid electrical system for studied UAVs.

Alongside the power sources mentioned previously, the system contains a MPPT (maximum power point tracker) for the solar cells' output. This maintains the solar cells at the maximum power point. The MPPT output and the battery are in parallel on the input of a DC/DC boost converter. This raises the output battery voltage from 24 VDC to 28 VDC—the value of the DC bus voltage. Both electric motors and other electrical consumer fed from this voltage are considered. The on-board electrical load is modelled by a variable resistor that follows the load profile. In the scheme, there are other components that permit us to measure voltages and currents at interesting points.

In order to simulate the electrical system's functioning, the components' parameters have to be specified. These parameters are presented in Table 6. Only the glider configuration and *Newsolar* configuration are considered here.

Table 6. Electrical system parameters.

	Glider	Newsolar
Number of solar cells	40 in series	4 groups in parallel, each one having 34 in series
Nominal voltage of the solar cells (V)	0.682	0.682
Current at 1000 W/m^2 solar radiation (A)	6.24	6.24
Battery nominal voltage (V)	24	24
Battery nominal capacity (Ah)	18	45
DC bus nominal voltage (V)	28	28

We also need to define a mission profile in order to obtain the system's behavior. It was mentioned that the *Newsolar* configuration is not designed to obtain a continuous flight performance. The authors seek to investigate the possibility of using use this configuration in daily missions, as long as solar radiation exists. It is considered that this UAV takes off at dawn and climbs, at the maximum climb speed allowed by the batteries, to 2000 m altitude. After that, it executes a horizontal flight all day long with the maximum speed allowed by the solar cells in the conditions mentioned previously. Even 30 min, the UAV executes maneuvers with maximum electrical motor power for 2 min. When the battery charging level drops under 23%, after sunset, the UAV descends along the minimum-gliding slope at a speed corresponding to the minimum power for horizontal flight. The consumed power in each phase and the time taken are presented in Table 2. The on-board equipment is considered consume the power specified in Table 2 continuously.

The horizontal flight–maneuver cycle is repeated 30 times throughout a summer day. Solar radiation over the course of a summer day at medium latitudes is shown in Figure 13. The final phase is considered as gliding from 2000 m to 0 m with the on-board systems in function.
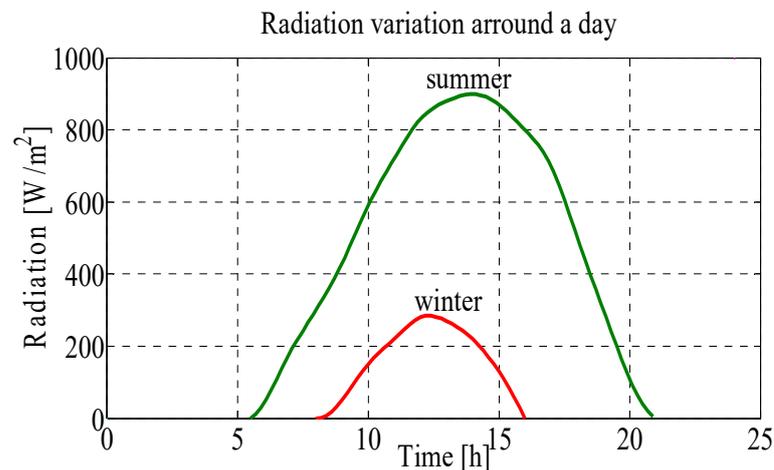
Figure 13. Solar radiation over the course of a summer day at medium latitudes.

With the load profile in Table 7 and system parameters in Table 6, we obtained by means of numerical simulations the results in Figure 14 for the glider configuration and the results in Figure 15 for the *Newsolar* configuration.

Table 7. Load profile of the considered mission.

Flight Phase	Glider		Newsolar	
	Power (W)	**Time (s)**	**Power (W)**	**Time (s)**
Take off	365	40	750	40
Climb to 2000 m	365	267	750	445
Horizontal flight	91	1800	325	1800
Maneuver	365	120	750	120
⋮	⋮		⋮	
Horizontal flight	91	1800	325	1800
Maneuver	365	120	750	120
Gliding	15	5000	50	1580
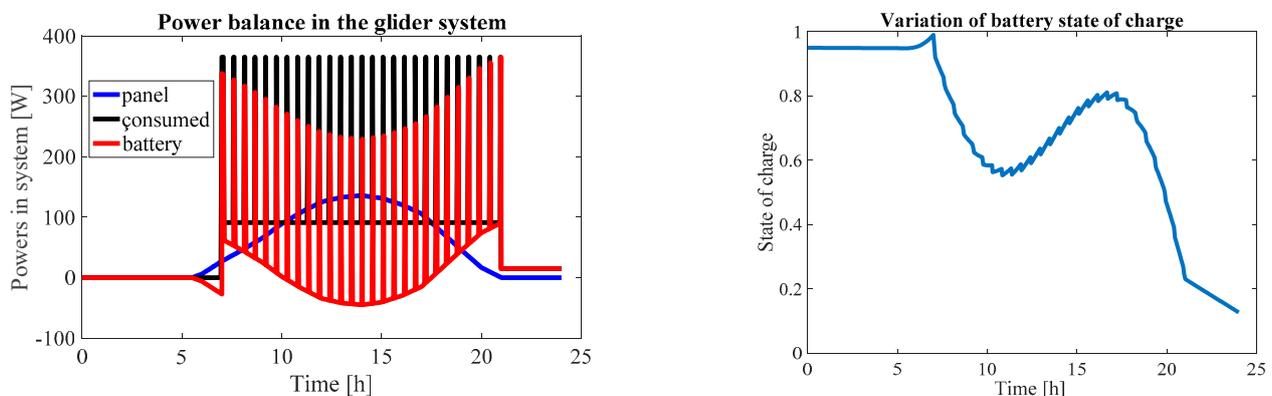
Figure 14. Electrical system behavior for glider configuration.
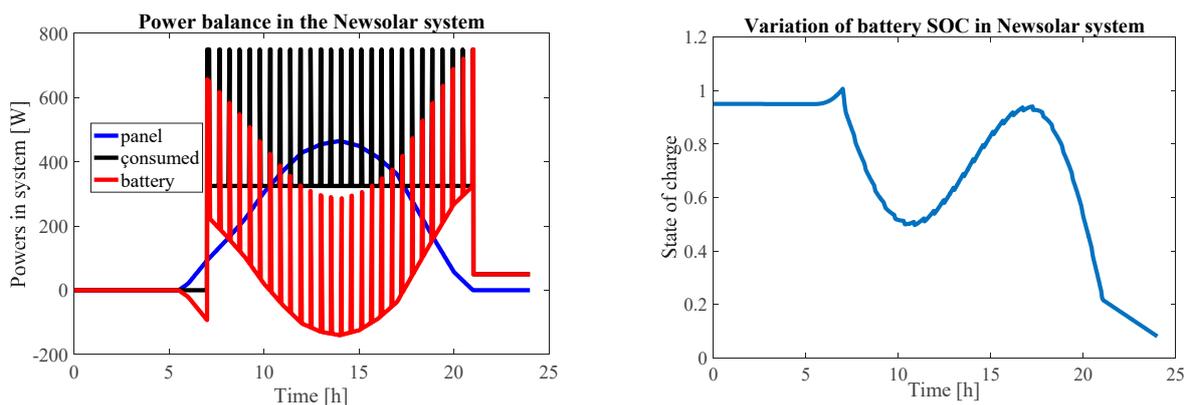
Figure 15. Electrical system behavior for *Newsolar* configuration.

It is noticed that both UAVs are capable of flight for the entire daylight period of the day at medium latitudes. The glider configuration is capable of executing a supplementary 45 min flight after sunset. The *Newsolar* configuration can fly only for 30 min after sunset. The estimated distance covered is around 1684 km for the glider configuration and 1132 km for the *Newsolar* configuration (around 67% of the distance).

The *Newsolar* configuration considered in this paper, compared to the glider configuration, is capable of carrying 250% larger payload, even though its fly speed is only around 70% of the glider configuration's fly speed. It also has a higher structural strength than the glider configuration. The energy consumed by the payload on board the *Newsolar*

configuration is 3 times greater than the energy consumed by the glider configuration. So, the *Newsolar* configuration, even though it has lower aerodynamic efficiency, is suitable for carrying a considerably larger payload with the same wingspan as the glider configuration. According to the estimations in this paper, a glider configuration required to carry a payload with the same characteristics as *Newsolar* needs to have a wingspan that is two times larger. It is true that the glider configuration scaled for this payload would obtain a higher fly speed and will cover a longer distance in the same time. However, there are many applications that do not require a very high fly speed. For example, some surveillance applications do not need a very high speed, while some sophisticated equipment may be required, which is heavier and consumes more energy. In agriculture, crop state observation can only be performed in the daytime and does not require a high fly speed. A smaller airplane which is easier to store and is capable of carrying a payload that permits a detailed observation, is therefore useful in this situation. In the energy industry, for high-voltage overhead lines inspection, it is useful to have a more maneuverable airplane that is not as influenced by the atmospheric currents as the glider configuration. These observations are currently obtained using multi-rotor drones, which have a considerably lower autonomy than solar aircraft. The geological observation of some areas requires more complex equipment that is heavier and consumes more energy. This is another possible application for this aircraft.

5. Conclusions

The *Newsolar* configuration is capable of fulfill a mission with a continuous flight throughout the daylight period of a summer day at medium latitudes with the profile proposed in Table 7. In these conditions, it can be said that the option to build UAVs with lower aerodynamic efficiency but with more electrical power obtained from solar cells is interesting. This kind of UAV is useful for missions that do not need continuous flight during the nighttime. The payload of *Newsolar* is 2.5 times heavier than that of the glider configuration and consumes nearly 3 times more electrical power. The wingspan is the same for both configurations, but the wing surface area and the surface area covered by solar cells are considerably larger. The general configuration of this UAV is more robust, with the same wingspan, but the UAV is 67% longer. The covered distance in this mission by *Newsolar* is 67% that covered by the glider configuration.

The performance of the scaled glider is estimated to be similar to that of the glider configuration. From this point of view, the scaled glider configuration is better. However, this UAV has twice the wingspan of *Newsolar*, a more elastic and vulnerable structure, and less maneuverability.

The main contribution of this work is providing a first study concerning the trade-off between the aerodynamic efficiency and amount of solar energy that can be obtained on board a UAV. A new solar airplane configuration is proposed, and it is compared with present existing solar airplane configuration. The possible performance that can be achieved by this configuration is compared with the performance of this existing solar airplane. This study should be followed by other detailed studies and a design phase for this configuration until it is ready to fly.

A conclusion mentioned at the end of Section 1 is that pure solar flight is not useful for commercial applications. It is more realistic to use hybrid propulsion with batteries and solar cells or batteries, solar cells and fuel cells on board. Solar energy is used in order to save as much as energy as possible from other sources, but it cannot provide the entire amount of energy needed for UAVs with other applications than breaking records.

It is important to note that the *Newsolar* configuration can be improved and optimized from different points of view and for different missions. This study simply highlights that this configuration, with less aerodynamic efficiency but with more solar energy produced on board, can be interesting for future applications.

References

1. Oettershagen, P.; Melzer, A.; Mantel, T.; Rudin, K.; Lotz, R.; Siebenmann, D.; Leutenegger, S.; Alexis, K.; Siegwart, R.A. Solar-Powered Hand-Launchable UAV for Low-Altitude Multiday Continuous Flight. In Proceedings of the 2015 IEEE International Conference on Robotics and Automation (ICRA), Seattle, WA, USA, 26–30 May 2015; pp. 3986–3993. [CrossRef]
2. Noth, A. Design of Solar Powered Airplanes for Continuous Flight. Doctor's Dissertation, ETH Zurich, Zurich, Switzerland, 2008.
3. Chu, Y.; Ho, C.; Lee, Y.; Li, B. Development of a Solar-Powered Unmanned Aerial Vehicle for Extended Flight Endurance. *Drones* **2021**, *5*, 44. [CrossRef]
4. Xu, Y.; Zhu, W.; Li, J.; Zhang, L. Improvement of endurace performance for high-altitude solar-powered airships: A review. *Acta Astronaut.* **2020**, *167*, 245–259. [CrossRef]
5. Yu, D.; Lv, X. Configuration analysis for high-altitude/long endurance airships. *Aircr. Eng. Aero. Technol.* **2010**, *82*, 147–164. [CrossRef]
6. Zhu, Y.; Guo, Z.; Hou, Z. Solar-powered airplanes: A historical perspective and future challenges. *Prog. Aerosp. Sci.* **2014**, *71*, 36–53. [CrossRef]
7. Leutenegger, S. Solar Aircraft—Design and Algorithms for Efficient and Robust Autonomous Operation. Doctor's Thesis, ETH Zurich, Zurich, Switzerland, 2014.
8. Plessis, F.; Meyer, J. Design considerations for long endurance unmanned aerial vehicle. In *Aerial Vehicles*; Intech: London, UK, 2009; ISBN 978-953-7619-41-1. [CrossRef]
9. Lisoski, D.; Tischler, M. Solar Powered Stratospheric Research Aircraft Flight test and System Identification. In Proceedings of the RTA Symposium on System Identification for Integrated Aircraft Development and Flight Testing, Paper #27, Madrid, Spain, 5–7 May 1998.
10. Müller, R.; Kiam, J.J.; Mothes, F. Multiphysical simulation of a semi-autonomous solar powered high altitude pseudo-satellite. In Proceedings of the IEEE Aerospace Conference, Big Sky, MT, USA, 3–10 March 2018; pp. 1–16. [CrossRef]
11. Ross, H. Fly Arround the World with a Solar Powered Airplane. In Proceedings of the 26th Congress of International Council of the Aeronautical Sciences (ICAS), Anchorage, AK, USA, 14–19 September 2008. AIAA 2008-8954.
12. National Research Council. *Uninhabited Air Vehicles: Enabling Science for Military Systems*; The National Academies Press: Washington, DC, USA, 2000. Available online: http://nap.nationalacademies.org/9878 (accessed on 15 November 2022). [CrossRef]
13. Mehta, A.; Yadav, S.; Solanki, K.; Joshi, C. Solar Aircraft—Future Need. *Int. J. Adv. Eng. Technol.* **2012**, *3*, 43–48.
14. Mobariz, K.; Ypussef, A.; Abdel-Rahman, M. Long endurance hybrid fuel cell—Battery powered UAV. *World J. Model. Simul.* **2015**, *11*, 69–80.
15. Lee, B.; Kwon, S.; Parl, P.; Kim, K. Active Power Management System for an Unmanned Aerial Vehicle Powered by Solar Cells, a Fuel Cell, and Batteries. *IEEE Trans. Aerosp. Electron. Syst.* **2014**, *50*, 3167–3177. [CrossRef]
16. Shiau, J.K.; Ma, D.M.; Yang, P.Y.; Wang, G.F.; Gong, J.H. Design of a Solar Power Management System for an Experimental UAV. *IEEE Trans. Aerosp. Electron. Syst.* **2009**, *45*, 1350–1360. [CrossRef]
17. Wang, H.; Shen, J. Analysis of the Characteristics of Solar Cell Array Based on MATLAB/Simulink in Solar Unmanned Aerial Vehicle. *IEEE Access Open J.* **2018**, *6*, 21195–21201. [CrossRef]
18. Mecrow, B.; Bennett, J.; Jack, A.; Atkinson, D.; Freeman, A. Drive Topologies for Solar-Powered Aircraft. *IEEE Trans. Ind. Electron.* **2010**, *57*, 457–464. [CrossRef]
19. Dai, Q.; Fang, X.; Li, X.; Tian, L. Performance simulation of high altitude scientific balloons. *Adv. Space Res.* **2012**, *49*, 1045–1052. [CrossRef]
20. Mueller, J.B.; Zhao, Y.J.; Garrard, W.L. Optimal ascent trajectories for stratospheric airships using wind energy. *J. Guid. Control Dyn.* **2009**, *32*, 1232–1245. [CrossRef]
21. Chu, X.; Lin, X.; Lan, W. Enegy-optimal rectilinear trajectory for stratospheric airships in constant wind field. In Proceedings of the 3rd IEEE Annual International Conference on Cyber Technology in Automation, Control and Intelligent Systems, Nanjing, China, 19–22 June 2013; pp. 264–269.
22. Dorobantu, A.; Murch, A.; Mettler, B.; Balas, G. Frequency domain system identification for a small, low-cost, fixed wing UAV. In Proceedings of the 2011 AIIA Guidance, Navigation and Control Conference, Portland, OR, USA, 8–11 August 2011; pp. 1–13.

23. Mohsan, S.A.H.; Othman, N.Q.H.; Li, Y.; AlSharif, M.; Khan, M.A. Unmanned aerial vehicles (UAVs): Practical aspects, applications, open challenges, security issues and future trends. *Intell. Serv. Robot.* **2023**, *16*, 109–137. [CrossRef] [PubMed]

24. Voinea, D.G. Possible configuration for a Solar Power UAV. In Proceedings of the EL-SES Conference, Craiova, Romania, 8–9 July 2022; pp. 1–6.